JOURNAL OF MATERIALS SCIENCE 29 (1994) 1724–1730

Creep of PE-10 nickel-base superalloy at 973 K

A. J. MARZOCCA
Universidad de Buenos Aires, Facultad de Ciencias Exactas y Naturales, Dto. de Física, Pabellón 1, Buenos Aires (1428), Argentina

A. C. PICASSO
Universidad del Centro de la Provincia de Buenos Aires, Facultad de Ciencias Exactas, IFIMAT, Pinto 399, Tandil, Prov. de Buenos Aires (7000), Argentina

Creep data, at 973 K and stresses between 355 and 512 MPa, in flat specimens of PE-10 nickel-base superalloy are reported. The data have been interpreted in terms of a constitutive equation based on a creep model involving dislocation climb and cross-slip over the strengthening phase. Strain-rate sensitivity and apparent activation energy have also been measured and analysed in the frame of the proposed model.

1. Introduction

In recent years, efforts have been made to explain the mechanisms that govern the plastic deformation in precipitation hardened alloys. One of the most important aspects of selecting a high-temperature and high-stress material is its creep resistance. Superalloys have been used typically as rotating blades of gas turbines, and creep deformation has been one of the most critical material properties to be considered [1].

The creep strengthening in superalloys has been explained by assuming that the dispersed second-phase particles act as obstacles to dislocation movement.

Several mechanisms have been proposed to explain the creep rate in these materials. Ansell and Weertman's paper [2] was the first to develop a theory about creep mechanisms in multiphase alloys. They suggest that the rate-controlling process is dislocation climb over the second-phase particles. At low stresses, they propose dislocation climb over particles with no pile-up or bowing of dislocations at the particles. In this case, the resolved steady state creep rate, $\dot{\gamma}$, changes linearly with the resolved shear stress, τ, following the law

$$\dot{\gamma} = \pi\tau \boldsymbol{b}^3 D/2kTh^2 \quad (1)$$

where h is the characteristic particle size, $\boldsymbol{b}$ the Burgers vector, D the self-diffusion coefficient, k the Boltzmann's constant and T the absolute temperature. At high stresses, greater than the Orowan stress, a dislocation will move past the particles by bowing out and pinching off loops around the particles. Now, the creep rate will be controlled by the rate at which the dislocation loop nearest to the particle climb to the top of the particle and is annihilated. Then, another loop will be moved inwards and it is possible to form a new loop by bowing and pinching off an arrested dislocation. The expression for this process is

$$\dot{\gamma} = 2\pi\tau^4\Gamma^2 D/hG^3kT \quad (2)$$

where Γ is the average distance between particles and G the shear modulus of the matrix.

At very high stresses, Ansell and Weertman propose an exponential relationship (without demonstration in their paper)

$$\dot{\gamma} = \tau^2(\pi\Gamma D/2G^2\boldsymbol{b}^2h)\exp(2\tau^2\Gamma\boldsymbol{b}^2/GkT) \quad (3)$$

with the condition that the second-phase particles are strong enough to withstand the stresses exerted by dislocations piled up against them.

Rowe and Freeman [3] studied deformation creep in M-252 and Inconel 700 superalloy. They found a dependence between the strain rate and the applied stress similar to Equation 2.

Wilcox and Clauer [4], assuming that the density of mobile edge dislocations depends on applied stress, σ, and utilizing Ansell and Weertman's model, obtain

$$\dot{\varepsilon} = A\sigma^n \quad (4)$$

where $\dot{\varepsilon}$ is the unresolved strain rate and $n = 5$. In general, A includes the Arrhenius coefficient, $\exp(-Q/kT)$, where Q is the activation energy of the principal process. A similar equation was used by Carey *et al.* [5] to build a deformation mechanism map for IN738LC superalloy.

Lagneborg [6] considers that Equations 1 and 2 do not agree with experimental data where the stress exponent is greater than 4. He introduces a back stress which the precipitated particles exert on a dislocation to solve the problem.

Depending on the kind of superalloy and the applied stress, n can vary between 4 and 16 and Q from 400–700 kJ mol^{-1}. This problem can be solved using an expression such as [6–17]

$$\dot{\varepsilon} = B(\sigma - \sigma_0)^n \exp(-Q_0/kT) \quad (5)$$

where the value of n over the whole range of stresses and temperatures lies between 3.5 and 4. In this case, Q_0 corresponds to the self-diffusion energy. σ_0, the friction stress, depends on stress, temperature and

0022–2461

structure [1]. Lagneborg and Bergman [11] propose a dependence between the effective stress ($\sigma - \sigma_0$) and the total dislocation density, ϕ, as

$$\sigma - \sigma_0 = A_1 G\boldsymbol{b}\phi^{1/2} \quad (6)$$

where A_1 is a constant.

The study of the activation parameters, Q and the strain-rate sensitivity, m, provides information about the kind of microscopic mechanisms that govern the deformation of the alloy.

Apparent activation energy is calculated as

$$Q = \partial \ln\dot{\varepsilon}/\partial(1/kT)|_{\sigma,S} \approx \Delta \ln\dot{\varepsilon}/\Delta(1/kT)|_{\sigma,S} \quad (7)$$

and it is measured by abrupt and small changes in temperature, in the steady-state creep region, at constant stress and structure, S.

Sensitivity, m, is defined as

$$m = \partial \ln\dot{\varepsilon}/\partial \ln\sigma|_{T,S} \approx \Delta \ln\dot{\varepsilon}/\Delta \ln\sigma|_{T,S} \quad (8)$$

and is measured at constant temperature and structure by abrupt changes of stress.

Mulford [18] studied the strengthening mechanism in different Inconel superalloy analysing the variation of m with stress. He evaluated the activation area associated with the deformation process, A^*, by means of the relationship

$$A^* = mkT/\boldsymbol{b}\sigma \quad (9)$$

At low temperatures (300 K), A^* increases with the γ' precipitate size for Inconel X750. As the average size of the precipitates increases, they begin to behave as relatively athermal obstacles. At high temperatures (950 K), the activation area decreases, and γ' precipitates may also be considered as athermal obstacles.

This paper presents creep data, at 973 K, of PE-10 nickel-base superalloy for various applied stresses. The results are interpreted in terms of a constitutive equation based on a creep model involving climb and cross-slip of dislocations. Activation energy and strain-rate sensitivity have been measured and analysed in the frame of the model.

2. Theory

There are several research works in the literature related to creep in superalloys which show an increase in the slope of the steady-state log σ–log $\dot{\varepsilon}$ curves at high stresses [1–4]. This behaviour could be analysed using, for example, Equation 5. However, it could be thought that there was more than one deformation mechanism acting on the material.

When we consider superalloy creep, dislocation climb over γ' and γ^* is mentioned as an important mechanism controlling strain rate. Weertman [2, 19–22] has proposed several creep models in which the creep strain is produced by glide of edge dislocations but the rate is controlled by the climb of such dislocations in order to surmount some types of barrier. In the case of superalloys, these barriers would be the dispersed second-phase particles [2].

In the range of high stresses, the climb velocity can be expressed as

$$v = [2\pi D/\boldsymbol{b}\ln(R/\boldsymbol{b})]\exp(N\tau\boldsymbol{b}A^*/kT) \quad (10)$$

where N is the number of piled-up dislocations over the obstacle. Following Balluffi and Seidman [23], each dislocation dominates a cylindrical region of outer radius R given by $R = (\pi\phi)^{-1/2}$. The self-diffusion coefficient is expressed as $D = D_0 \exp(-U/kT)$, where U is the self-diffusion energy and D_0 the pre-exponential term. The total number of dislocations in the pile-up is [24], therefore

$$N = \pi(1 - \eta)\Gamma\tau/G\boldsymbol{b} \quad (11)$$

where η is Poisson's ratio of the material. Then, from Equation 10

$$v = [2\pi D/\boldsymbol{b}\ln(R/\boldsymbol{b})] \times \exp[\pi(1 - \eta)\Gamma A^*\tau^2/GkT] \quad (12)$$

Following Ansell and Weertman [2], the strain rate could be expressed as

$$\dot{\gamma} = 1.5(\boldsymbol{b}/hd)v \quad (13)$$

where d is the distance a pinched-off loop must climb before another loop can be pinched off. This parameter is of the order

$$d = G\boldsymbol{b}/n\tau \quad (14)$$

By combining Equations 11, 12, 13 and 14 we obtain for the creep rate

$$\dot{\gamma} = \frac{3\pi^2}{\ln(R/\boldsymbol{b})}\frac{(1 - \eta)\Gamma D}{h\boldsymbol{b}^2G^2}\tau^2 \times \exp[\pi(1 - \eta)\Gamma A^*\tau^2/GkT] \quad (15)$$

If unresolved strain rates, $\dot{\varepsilon}_c$, and stresses are used, Equation 15 can be written as

$$\dot{\varepsilon}_c = \frac{3\pi^2}{42^{1/2}\ln(R/\boldsymbol{b})}\frac{(1 - \eta)\Gamma D}{h\boldsymbol{b}^2G^2}\sigma^2 \times \exp[\pi(1 - \eta)\Gamma A^*\sigma^2/4GkT] \quad (16)$$

In their investigations on thoriated nickel. Wilcox and Clauer [4] found cross-slip of dislocations around ThO_2 particles at 450 °C and they proposed this mechanism as responsible for plastic deformation at temperatures below 0.5 T_m. By-pass of particles by cross-slip is quite rare in superalloys because of the low stacking fault energy, f, of the matrix [1]. However, values between 90 and 450 erg cm^{-2} are reported in literature for nickel [4, 22, 25–27] at room temperature and lower values were found at elevated temperatures [4] which could explain the activation of cross-slip mechanisms.

As Nichols points out in his paper about activation area for creep [28], in the most important theories of steady-state creep of metals, glide of both edge and screw dislocations is completely ignored.

Poirer [29] developed a steady-state creep model considering that dislocation climb and cross-slip are the mechanisms that control the plastic deformation at intermediate temperatures. The two mechanisms work in a simultaneous way and the steady-state

strain rate can be expressed as

$$\dot{\varepsilon} = \dot{\varepsilon}_{cs} + \dot{\varepsilon}_c \quad (17)$$

where $\dot{\varepsilon}_{cs}$ is the contribution due to dislocation cross-slip.

We could consider the same two processes acting when the dislocation loop is not blocked by the stress field produced by the interaction with another one, but by the interaction with the second-phase particle. Both dislocation climb and cross-slip over the particles are accepted mechanisms that could control the deformation processes in dispersion-hardened alloys [30].

Poirer [29] considers that cross-slip is controlled by the thermally activated constriction of the stacking fault and recombination of the partial dislocations. He obtains

$$\dot{\gamma}_{cs} = A(\tau/G)^2 \exp(-Q_{cs}(\tau, f)/kT) \quad (18)$$

where A is a constant and Q_{cs} is the activation energy of cross-slip, a function of the stress and the stacking fault energy. Escaig [31] has calculated an expression, at first order in τ, for Q_{cs} as

$$Q_{cs} = (G^2\boldsymbol{b}^4/Cf)\,[\ln(G\boldsymbol{b}/C_l f)]^{1/2} \times [1 - (3\boldsymbol{b}\tau/f)] \quad (19)$$

where $C = 1859.82$ and $C_l = 14.51$.

Then, using Equations 18 and 19 we obtain

$$\dot{\gamma}_{cs} = A(\tau/G)^2 \exp(-\delta/kT) \times \exp(3\boldsymbol{b}\tau\delta/fkT) \quad (20)$$

with

$$\delta = (G^2\boldsymbol{b}^4/Cf)[\ln(G\boldsymbol{b}/C_l f)]^{1/2} \quad (21)$$

Equation 20 can be rewritten as

$$\dot{\gamma}_{cs} = \dot{\varepsilon}_0 \tau^2 \exp(\beta\tau) \quad (22)$$

with

$$\dot{\varepsilon}_0 = (A/G^2)\exp(-\delta/kT) \quad (23)$$

$$\beta = 3\boldsymbol{b}\delta/fkT \quad (24)$$

and if unresolved strain rates and stresses are used

$$\dot{\varepsilon}_{cs} = \frac{\dot{\varepsilon}_0}{4\,2^{1/2}} \sigma^2 \exp(\beta\sigma/2) \quad (25)$$

If we consider that dislocation climb can be expressed using Equation 16, we will write the steady-state creep rate, Equation 17, as

$$\dot{\varepsilon} = (1/4\,2^{1/2})\sigma^2 [\dot{\varepsilon}_0 \exp(\beta\sigma/2) + \dot{\varepsilon}_1 \exp(\alpha\sigma^2/4)] \quad (26)$$

where

$$\dot{\varepsilon}_1 = 3\pi^2(1 - \eta)\Gamma D/\ln(R/\boldsymbol{b})G^2\boldsymbol{b}^2 h \quad (27)$$

$$\alpha = \pi(1 - \eta)\Gamma A^*/GkT \quad (28)$$

On differentiating Equation 26 it is easy to show that the parameter m, defined by Equation 8, is given by

$$m = 2 + 1/2(\dot{\varepsilon}_c/\dot{\varepsilon})\alpha\sigma^2 + 1/2(\dot{\varepsilon}_{cs}/\dot{\varepsilon})\beta\sigma \quad (29)$$

This Equation shows that m depends on the applied stress, on the strain rate and parameters of the model.

3. Experimental procedure

3.1. Material

The specimens were obtained from a PE-10 superalloy air cast by the investment casting process in the Solidification Laboratory, IFIMAT, UNCPBA (Tandil, Argentina) [32, 33]. The composition of the alloy is given in Table I. This material is based on the EPE-10 alloy, mentioned in Haynes' work [34].

Before performing the creep test, as-cast samples were heat treated in an argon atmosphere with solution treatment for 10 h at 1373 K, water quenched, and a precipitation treatment for 16 h at 1023 K, water quenched. Metallographic observations of the specimens were made by transmission electron microscopy (TEM), using the experimental procedure given elsewhere [35]. The microstructure observed

TABLE I Composition of the superalloy PE-10 (wt %)

C	0.02
Mn	0.28
Si	0.34
Cr	10.90
Ni	Bal.
Mo	5.90
W	2.35
Co	< 0.10
Fe	2.55
Nb/Ta	6.73
Al	0.17
Cu	< 0.20
P	< 0.03
S	< 0.005

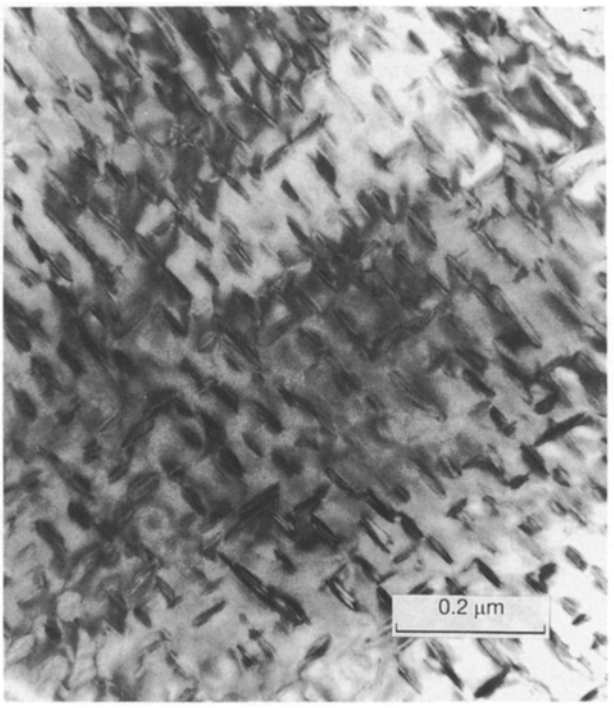

Figure 1 Transmission electron micrograph of PE-10 showing γ* plates.

showed an austenitic matrix containing γ^* (Ni_3Nb) type precipitates into the grain and over grain boundaries (Fig. 1). It has been shown that austenitic Ni–Fe–Cr–Nb alloys containing more than about 30 wt% Ni may be age hardened, with a Ni_3Nb phase as the major hardening precipitate [35, 36].

On the other hand, the carbide fraction volume was disregarded owing to the low carbon content in this alloy. The average grain size was 85 μm.

3.2. Creep tests

The creep tests were performed at the Laboratory of Mechanical Properties of Metals, IFIMAT, UNCPBA (Tandil, Argentina). They were carried out on planar samples with an average cross-section of $3.65 \pm 0.16\ mm^2$ and 18.25 mm gauge length. They were performed in air with a loading beam capable of maintaining a constant stress, within 1% of the initial stress, up to strains of the order of 10% [37, 38].

The experiments were performed at 973 K. The temperature was regulated by a proportional derivative controller. Thermocouples were attached to the grips and the fluctuations were kept below $\pm$ 1 K during the whole experiment.

The elongation of the specimen was measured by attaching fused silica rods, which extended out of the furnace, to the upper and lower grip. Because the lower grip was fixed, measurement of the relative displacement of the fused silica rods, using LVDT, gives the true elongation of the specimen, eliminating any influence of the loading train. Experimental details are given elsewhere [38].

4. Results

Fig. 2 shows the creep strain as function of time for stresses between 355 and 512 MPa at 973 K. These results suggest the usual separation between transient or primary and secondary or steady-state creep, because the strain rate decreases to a constant value at all the stresses.

When the data are plotted as log σ versus log $\dot{\varepsilon}$ for the steady-state creep, we obtain the graph of Fig. 3. In this plot, $\dot{\varepsilon}$ has been obtained by calculating the derivatives of the curves of Fig. 2 in the steady-state region, and plotting them as function of the corresponding stress.

Fig. 3 shows typical behaviour observed in many superalloys in which the slope of the log σ versus log $\dot{\varepsilon}$ curve increases at high values of stress [1]. In our graph, there are two regions with different slopes (approximately 3.7 and 8.9). These values agree with the behaviour of other nickel-base superalloys in creep [1] and, in this frame, it could imply that more than one mechanism controls the creep deformation depending on the stress level.

It was possible to measure the sensitivity, m, at different stress levels by making a small change in the applied stress ($\Delta\sigma \approx \pm 0.1\ \sigma$) and using Equation 8, evaluating the strain rate before and after the change. Once the equilibrium value was obtained for the new stress level, we returned to the original stress, and therefore the value of m could be obtained by increasing or decreasing the stress. The values obtained are given in Table II where the stresses measured before the small change are also indicated. All the measurements were performed in the steady-state region of the strain versus time curve.

The apparent activation energy, Q, was also measured by abrupt and small changes in temperature ($\Delta T = \pm 20$ K) at various stresses in the steady-state region. The values obtained are given in Table III where the stress levels are also indicated.

5. Discussion

The behaviour of steady state creep of this superalloy can be studied using the model proposed in

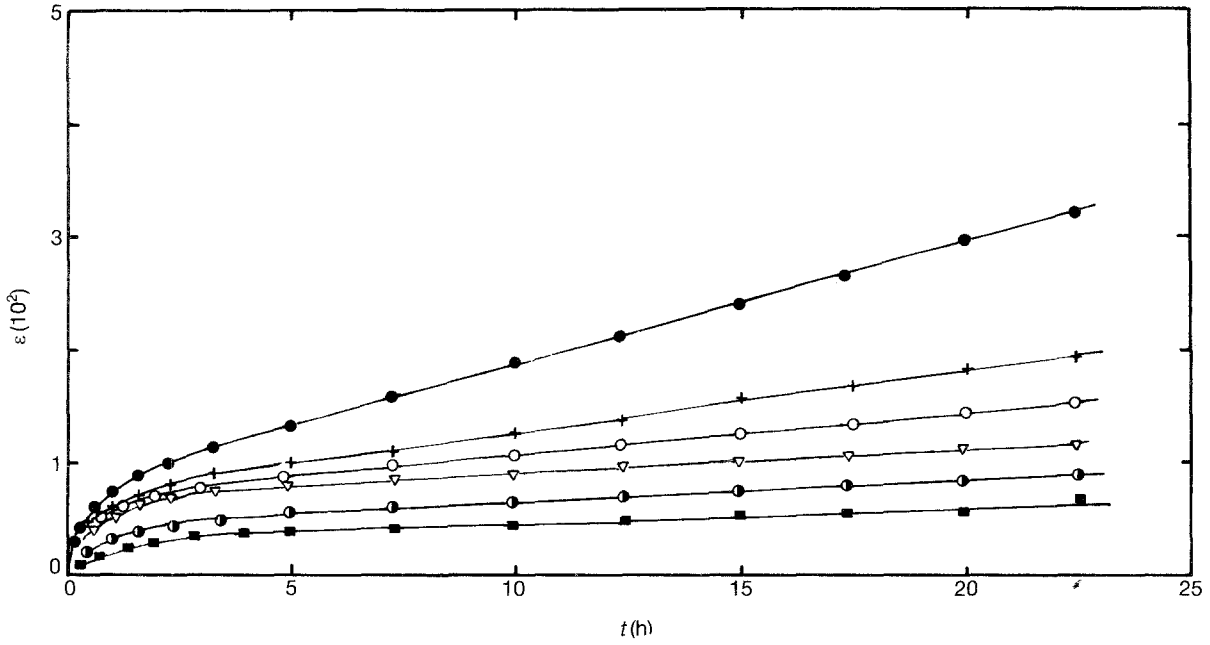

Figure 2 Creep strain as a function of time at 973 K and various stresses for PE-10 nickel-base superalloy. (■) 355.0 MPa, (◑) 368.0 MPa, (▽) 401.9 MPa, (○) 449.0 MPa, (+) 493.0 MPa, (●) 512.0 MPa.

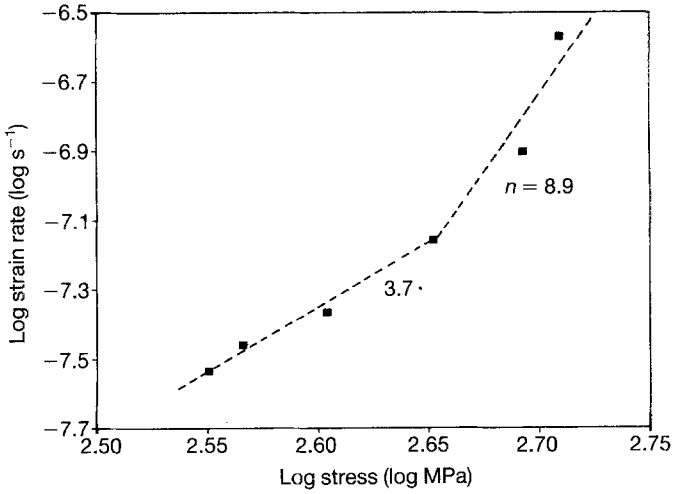

Figure 3 Log σ versus log ε̇ for steady-state creep for PE-10 nickel-base superalloy at 973 K, obtained from Fig. 2. Two regions of different slope are shown.

TABLE II The parameter m given by Equation 8 measured at various stresses

σ(MPa)	m
355.0	9.4
396.0	5.8
401.9	3.0
429.9	7.5
449.7	8.8
475.7	5.8
493.0	10.5
512.0	19.7
522.0	12.1

TABLE III Apparent activation energy, Q, for steady-state creep of PE-10, obtained by making changes in temperature of ± 20 K. Subscript 1 indicates that the values were obtained on increasing the temperature and subscript 2 on decreasing it

σ(MPa)	Q_1(kJ mol^{-1})	Q_2(kJ mol^{-1})
355.0	390.0	362.0
368.0	454.3	–
373.0	251.0	–
401.9	469.7	402.7
449.7	554.3	475.2
512.0	402.7	–

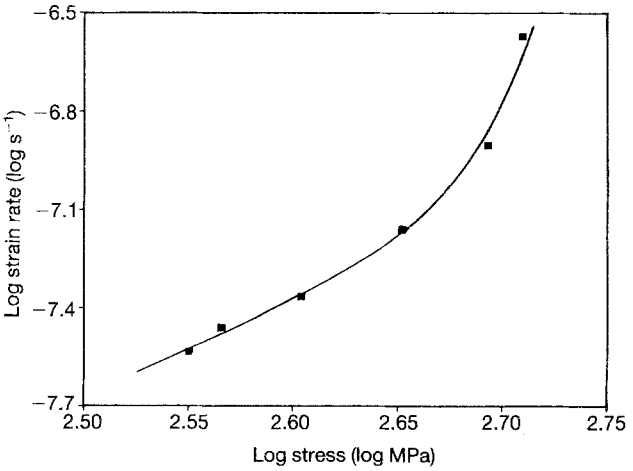

Figure 4 Comparison of stress versus strain-rate curves of (■) experimental data and (——) the theoretical curve predicted by Equation 26 for steady-state creep of PE-10 at 973 K.

TABLE IV Material data for PE-10 superalloy

		Reference
$\boldsymbol{b}$(m)	2.49×10^{-10}	[26]
G [Pa]	$7.87 \times 10^{10} \exp\{-3.7\,10^{-4}(T-300)\}$	[39]
η	0.31	[40]
D_0(m^2 s^{-1})	1.27×10^{-4}	[41]
U(kJ mol^{-1})	281.35	[41]

Section 2. In fact, experimental strain-rate data can be fitted, in the range of stresses considered, using Equation 26 with $\dot{\varepsilon}_1 = 4.0 \times 10^{-29}$ s^{-1} Pa^{-2}, $\alpha = 17.2 \times 10^{-17}$ Pa^{-2}, $\dot{\varepsilon}_0 = 5.6 \times 10^{-25}$ s^{-1} Pa^{-2}, $\beta = 4.9 \times 10^{-9}$ Pa^{-1}.

In Fig. 4 the fitting between the experimental points and the theoretical model expressed by Equation 26 is very good within experimental error.

Using the relationship given in Equations 24, 27 and 28, some parameters related to microstructure of the material can be estimated. The material data for the matrix of the alloy are listed in Table IV.

If we consider that $A^* \approx \boldsymbol{b}^2$ and this is replaced in Equation 28, using the value of α presented, we will obtain a value of Γ which is higher than that estimated by TEM (Fig. 1). However, Nichols [28] in his review about activation area in creep deformation, points out the magnitude of A^* may well be substantially larger than $\boldsymbol{b}^2$ if the process is controlled by diffusion. Li [42] and Balusubramanian *et al.* [43] have calculated activation areas in several materials, yielding values ranging from several thousands of $\boldsymbol{b}^2$ at low stresses and a few tens of $\boldsymbol{b}^2$ at high stresses. In order to estimate the activation area in our material, we can consider, from Fig. 1, a mean distance between precipitates of the order of 3×10^{-8} m. Then using the value of α, the data in Table IV and Equation 28 we obtain $A^* \approx 35\,\boldsymbol{b}^2$, which is consistent with the activation area obtained in several metals [28, 42, 43] and nickel-base superalloys [18].

If the experimental value of $\dot{\varepsilon}_1$ is used in Equation 27 and considering $\ln(R/b) \approx 3.12$ (considering a typical dislocation density of $10^{12}\,cm^{-2}$ [23]) a value of $\Gamma/h \approx 1.4$ will be obtained. This relationship shows that the values of the mean distances between precipitates and the characteristic size of these have similar values. This assertion is confirmed by the distribution of precipitates observed in Fig. 1, where the sizes of the plates are similar to the mean separation between the second-phase particles.

The value of β makes it possible to estimate the stacking fault energy of the matrix. From Equations 21 and 24, f can be obtained by solving the relationship

$$f^2 = 0.0885\,[\ln(1.053/f)]^{1/2}$$

The solution of this Equation gives $f = 0.313\ J\,m^{-2}$, which is a value within the range reported in the literature for nickel [4, 21, 25–27] and nickel-base superalloys [18, 44].

Using the experimental results presented in Table III, a mean value of $Q = 428.9\ kJ\,mol^{-1}$ is obtained. This value agrees with the apparent activation energies observed in several superalloys [1]. The value of our superalloy is much larger than the self-diffusion energy of the matrix given in Table IV. However, if we wanted to analyse the meaning of the apparent activation energy, we would consider the result in the frame of the proposed deformation model in which the contribution of Q_{cs} would be important. In this context, Q will be higher than U [45].

We can use the parameters $\dot{\varepsilon}_1$, α, $\dot{\varepsilon}_0$ and β to evaluate the sensitivity, m, by means of Equation 29. In Fig. 5 the experimental data agreement between the measured values and those predicted by the theoretical model is good if we consider that we are evaluating the derivative of the steady-state behaviour. The behaviour of the experimental point at 355 MPa is doubtful, because in this case the change in σ used to obtain m was not so small ($\approx$40 MPa). We can consider that the tendency of the experimental data is that of the theoretical model.

Finally, the results of m given in Table II are in the range of the experimental values of other superalloys studied at temperatures where diffusion processes are important [1, 15, 18].

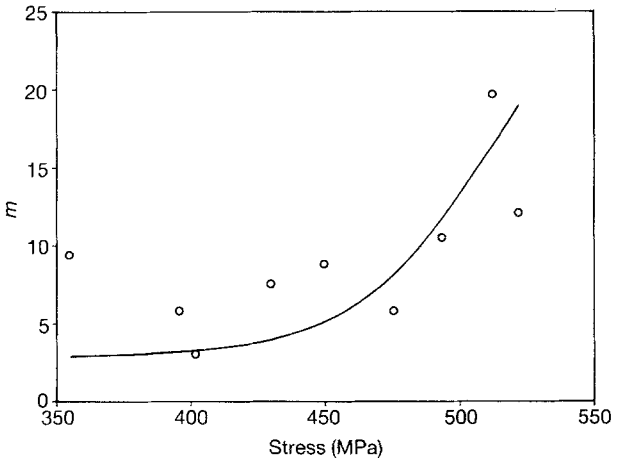

Figure 5 Variation of the sensitivity, m, with stress. Comparison between (○) experimental data and (——) the theoretical relationship of Equation 29.

6. Conclusions

The steady-state creep characteristics of PE-10 nickel-base superalloy, at 973 K, are presented. They are described by a model which considers dislocation climb over the second-phase particles and cross-slip. Using the experimental data, some parameters of the model are evaluated: the ratio of the mean distance of precipitates to their characteristic size (Γ/h) and the activation area associated with the climb process. An estimation of the stacking fault energy is also made. This value agrees with the values presented in the literature.

Experimental data of m show a dependence on stress. They are compared with the estimated values using the theoretical model.

Finally, the apparent activation energy is evaluated, its value being similar to the results presented in the literature for other nickel-base superalloys.

Acknowledgements

We thank Dr Valentino Lupinc and Ing. Maurizio Maldini (ITM, CNR, Milano, Italy) for the helpful discussions and the electron micrographs, Dr Hugo A. Palacio (Solidification Laboratory, UCPBA, Tandil, Argentina) who provided the materials used in this research, and Dr Fransico Povolo for helpful advice. The authors also thank M. E. Rodriguez for her co-operation. This work was supported in part by the IFIMAT, Faculty of Science, University of the Centre of Buenos Aires State.

References

1. V. LUPINC, in "Proceedings on High Temperature Alloys for Gas Turbines", Liege, 1982, edited by B. R. Brunetaud, D. Coutsouradis, T. B. Gibbons, Y. Lindblom, D. B. Meadowcroft and R. Stickler (Reidel, London, 1982) p. 398.
2. G. S. ANSELL and J. WEERTMAN, *Trans. Met. Soc. AIME* **215** (1959) 838.
3. J. P. ROWE and J. W. FREEMAN, in "Proceedings of the Joint International Conference on Creep" (Institute of Engineering, London, 1963) p. 1.
4. B. A. WILCOX and A. H. CLAUER, *Trans. Met. Soc. AIME* **236** (1969) 578.
5. J. A. CAREY, P. M. SARGENT and D. R. H. JONES, *J. Mater. Sci. Lett.* **9** (1990) 572.
6. R. LAGNEBORG, *J. Mater. Sci.* **3** (1968) 596.
7. K. R. WILLIAMS and B. WILSHIRE, *Met. Sci. J.* **7** (1973) 176.
8. J. D. PARKER and B. WILSHIRE, *ibid.* **9** (1975) 248.
9. W. J. EVANS and G. F. HARRISON, *ibid.* **10** (1976) 307.
10. J. P. DENNISON, P. D. HOLMES and B. WILSHIRE, *Mat. Sci. Eng.* **33** (1978) 35.
11. R. LAGNEBORG and B. BERGMAN, *Met. Sci.* January (1976) 20.
12. W. J. EVANS and G. F. HARRISON, *ibid.* November (1979) 641.
13. T. B. GIBBONS, *Scripta Metall.* **12** (1978) 749.
14. W. J. PLUMBRIDGE and R. A. BARLETT, *Res. Mech.* **3** (1981) 299.
15. O. AJAJA, T. E. HOWSON, S. PURUSSHOTHAMAN and J. K. TIEN, *Mater. Sci. Eng.* **44** (1980) 165.
16. W. J. EVANS, A. W. BEALE and G. F. HARRISON, *Scripta Metall.* **14** (1980) 165.

17. T. L. LIN and M. WEN, *Mater. Sci. Eng.* **A128** (1990) 23.
18. R. A. MULFORD, *Acta Metall.* **27** (1979) 1115.
19. J. WEERTMAN, *J. Appl. Phys.* **21** (1955) 1213.
20. *Idem, ibid.* **28** (1957) 362.
21. *Idem, Trans. Met. Soc. AIME* **233** (1965) 2069.
22. *Idem, Trans. Am. Soc. Metals* **61** (1968) 681.
23. R. W. BALLUFFI and D. N. SEIDMAN, *J. Appl. Phys.* **36** (1965) 2708.
24. J. HIRTH and J. LOTHE, "Theory of dislocations" (McGraw-Hill, New York, 1968) p. 704.
25. I. L. DILLAMORE and R. E. SMALLMAN, *Philos. Mag.* **11** (1965) 191.
26. J. FRIEDEL, "Dislocations" (Addison-Wesley, London, 1964).
27. P. C. J. GALLAGHER, *Metall. Trans.* **1** (1970) 2429.
28. F. A. NICHOLS, *Mater. Sci. Eng.* **8** (1971) 108.
29. J. P. POIRER, *Rev. de Phys. Appl.* **11** (1976) 731.
30. P. B. HIRSCH, in "Rate Process in Plastic Deformation of Materials", Proceedings from the John E. Dorn Symposium, Cleveland, 1972, edited by J. C. M. Li and A. K. Mukherje (ASM no. 4, 1975) p. 1.
31. B. ESCAIG, *J. Phys. Fr.* **29** (1968) 225.
32. H. A. PALACIO, O. GARBELLINI, A. GES, R. SCARPA, A. PICASSO and H. BILONI, *Metal. Moderna*, in press (1993).
33. A. C. PICASSO and H. A. PALACIO, in "Proceedings Asociación Física Argentina VI", Vol. 1, San Luis, 1989, edited by Zagier and Urruty (Tandil, 1990) p. 208.
34. F. G. HAYNES, *J. Inst. Metals* **90** (1961) 311.
35. I. KIRMAN and D. H. WARRINGTON, *Metal. Trans.* **1** (1970) 2667.
36. I. KIRMAN, *J. Iron Steel Inst.* **207** (1969) 1612.
37. A. J. MARZOCCA, PhD Thesis, FCEN, University of Buenos Aires (1986).
38. A. C. PICASSO, Master Thesis, Faculty of Science, University of the Center of Buenos Aires State, Tandil (1990).
39. C. J. CAPITANI, private communication (1992).
40. H. KUCHLING, in "Taschenbuck der Physik" (Vergland Arri Deudsch, Frankfurt, 1988) p. 591.
41. M. BADIA and A. VIGNES, *Acta Metall.* **17** (1969) 177.
42. J. C. M. LI, in "Kinetics and dynamics in dislocation plasticity", edited by A. R. Rosenfield *et al.*, Dislocation Dynamics (McGraw-Hill, New York, 1968) p. 87.
43. N. BALUSUBRAMANIAN and J. C. M. LI, *J. Mater. Sci.* **5** (1970) 434.
44. A. J. ARDELL, V. MUNJAL and D. J. CHELLMAN, *Metall. Trans.* **7A** (1976) 1263.
45. A. J. MARZOCCA and A. C. PICASSO, to be published.

Received 7 September 1992
and accepted 27 September 1993